crystals

MDPI

Article

New Acetylenic Amine Derivatives of 5,8-Quinolinediones: Synthesis, Crystal Structure and Antiproliferative Activity

Monika Kadela-Tomanek [1,*], Maria Jastrzębska [2,3], Ewa Bębenek [1], Elwira Chrobak [1], Małgorzata Latocha [4], Joachim Kusz [5], Dorota Tarnawska [3,6] and Stanisław Boryczka [1]

1 Department of Organic Chemistry, School of Pharmacy with the Division of Laboratory Medicine in Sosnowiec, Medical University of Silesia in Katowice, 4 Jagiellońska Str., 41-200 Sosnowiec, Poland; ebebenek@sum.edu.pl (E.B.); echrobak@sum.edu.pl (E.C.); boryczka@sum.edu.pl (S.B.)
2 Department of Solid State Physics, Institute of Physics, University of Silesia, 4 Uniwersytecka Str., 40-007 Katowice, Poland; maria.jastrzebska@us.edu.pl
3 Silesian Center for Education and Interdisciplinary Research, University of Silesia, 75 Pułku Piechoty 1, 41-500 Chorzów, Poland; dorota.tarnawska@us.edu.pl
4 Department of Cell Biology, School of Pharmacy with the Division of Laboratory Medicine in Sosnowiec, Medical University of Silesia in Katowice, 8 Jedności Str., 41-200 Sosnowiec, Poland; mlatocha@sum.edu.pl
5 Department of Physics of Crystals, Institute of Physics, University of Silesia, 4 Uniwersytecka Str., 40-007Katowice, Poland; joachim.kusz@us.edu.pl
6 Department of Biophysics and Molecular Physics, Institute of Physics, University of Silesia, 4 Uniwersytecka Str., 40-007 Katowice, Poland
* Correspondence: mkadela@sum.edu.pl; Tel.: +48-323641666

Academic Editor: Sławomir J. Grabowski
Received: 20 December 2016; Accepted: 4 January 2017; Published: 7 January 2017

Abstract: Acetylenic amine derivatives of the 5,8-quinolinedione were synthesized and characterized by the ^{1}H and ^{13}C NMR, IR spectroscopy and MS spectra. Additionally, the 6- and 7-substituted allylamine-5,8-quinolinediones were synthesized for comparison purposes. The crystal structure was determined for the 6-chloro-7-propargylamine-5,8-quinolinedione and 7-chloro-6-propargylamine-5,8-quinolinedione. Additionally, the IR spectral analysis supplemented by the density functional theory (DFT) calculations were carried out. It was found that different positions of the propargylamine side chain had a distinct influence on crystal structure, formation of H-bonds and the carbonyl stretching IR bands. Correlation between the frequency separation $\Delta\nu$ of the carbonyl IR bands and the position of the 6- and 7-substituents was found. The 7-substituted derivatives exhibited a higher frequency separation $\Delta\nu$. The observed correlation could provide an opportunity to use the IR spectroscopy to study substitution reactions. Cytotoxic activities against three human cancer cell lines for the 5,8-quinolinedione derivatives with different amine substituents, i.e., propargylamine, *N*-methylpropargylamine, 1,1-dimethylpropargylamine, allylamine and propylamine were also analysed with respect to their molecular structure.

Keywords: propargylamine-5,8-quinolinediones; crystal structure; H-bonding; IR carbonyl bands

1. Introduction

The 5,8-quinolinedione derivatives were among the first compounds to be systematically modified in order to find products with higher biological activities, such as anticancer, anti-inflammatory or antibacterial [1–9]. For example, it was found that substitution of the electron-withdrawing groups at the 6- or 7-positions of the 5,8-quinolinedione led to an increase in the DNA degradation [8–13].

There are many reports on the synthesis, structure and biological activity of the amine derivatives of 5,8-quinolinedione, whereas studies on the alkyne amino analogues are very scarce [14]. Natural and synthetic acetylenic derivatives of the quinoline attract increasing attention since many of them display wide biological activity spectra [15–22]. According to the literature data, introduction of the alkyne group may significantly improve biological activity of these compounds [21,22].

In this study, we present synthesis and antiproliferative activity of the series of acetylenic amino derivatives of the 5,8-quinolinedione. Moreover, the structural properties of two acetylenic compounds, i.e., 6-chloro-7-propargylamine-5,8-quinolinedione and7-chloro-6-propargylamine-5,8-quinolinedione were determined by X-ray diffraction and IR spectroscopy.

Our attention was also focused on the carbonyl stretching bands in the infrared spectra of the propargylamine-substituted 5,8-quinolinedione, which are known as bands very sensitive to morphology. For para-quinones, one or two carbonyl bands can be observed. This feature can be influenced by many factors: mainly intra- and intermolecular interactions and conformational changes [23,24]. It can create the opportunity for additional structural investigations using IR carbonyl bands. For example, we recently found an interesting correlation between the frequency separation of carbonyl bands and the position of propylamine substituents on 5,8-quinolinediones [25]. Therefore, in this report we also aimed to check whether a similar correlation exists for the propargylamine-substituted 5,8-quinolinediones.

2. Results and Discussion

2.1. Chemistry

The 6,7-dichloro-5,8-quinolinedione **1** was prepared by the oxidation of the 8-hydroxyquinoline [12] and used as a starting compound for the synthesis of the acetylenic derivatives **2–3** using procedures described in the literature [8,9,25]. Treatment of compound **1** with the corresponding amine in tetrahydrofuran in the presence of potassium carbonate at room temperature gave a mixture of 7- and 6-aminosubstituted derivatives, **2a–e** and **3a–e**, respectively (Scheme 1).

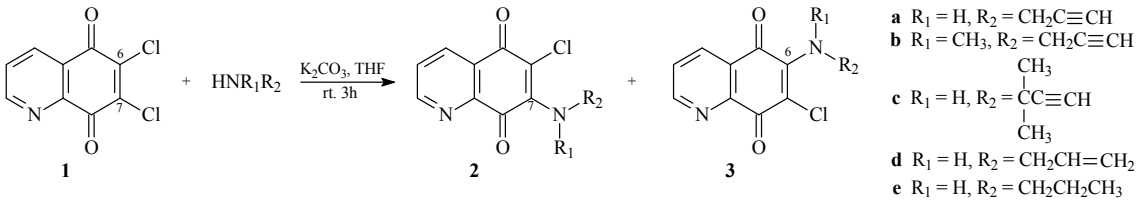

Scheme 1. Synthesis of the 6-chloro-7-substituted 5,8-quinolinediones **2a–e** and 7-chloro-6-substituted 5,8-quinolinediones **3a–e**.

The obtained mixtures were separated by column chromatography to afford pure products **2a–e** and **3a–e** with the 68%–58% and 16%–21% yields, respectively. The structures of all derivatives **2–3** were determined by the ^{1}H, ^{13}C NMR, IR and MS spectra.

For both isomeric compounds **2** and **3** the ^{1}H NMR chemical shifts were similar, and therefore it was not possible to distinguish between 6- and 7-substituents based on the spectra (see Figure S1–S8 in supplement material). According to the literature data [8,12], such differentiation is possible when using the ^{13}C NMR spectra. It was found that the isomers **2** and **3** showed different signal intensities of the C-5, C-8, C-6 and C-7 atoms. For the 6-aminosubstituted derivatives, the signal intensities of the C-5 and C-7 atoms were higher than those for the C-8 and C-6 atoms. For the 7-aminosubstituted derivatives, the signal intensities followed the opposite relation, i.e., they were higher for the C-8 and C-6 atoms. Therefore, it was confirmed that compounds **2** and **3** possessed the amine group at the C-7 and C-6 positions, respectively. Additionally, for derivatives **2a** and **3a**, the X-ray diffraction analysis confirmed also substitution of the propargylamine chain at the C-7 and C-6 positions, respectively.

2.2. Crystal Structure and Formation of Hydrogen Bonds

The 6-chloro-7-propargylamine-5,8-quinolinedione **2a** and 7-chloro-6-propargylamine-5,8-quinolinedione **3a** crystallized in two different monocyclic space groups, i.e., Pc and $P2_1/n$, respectively. Figure 1 shows molecular structures and atom numbers of the compounds **2a** and **3a**. In Table 1, the crystal parameters, experimental data and refinement details are shown.

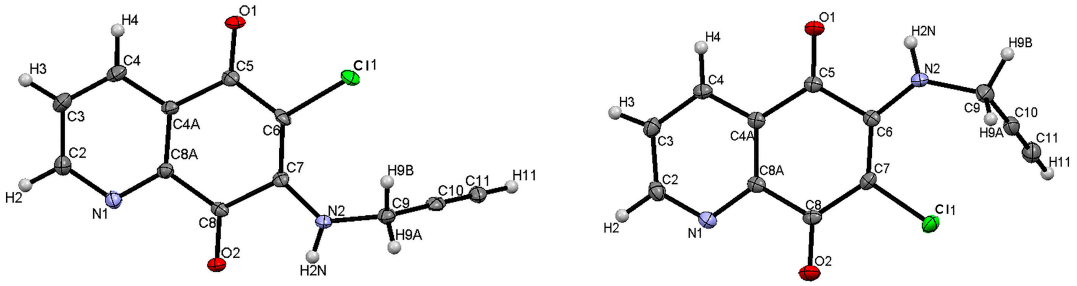

Figure 1. Molecular structures with atom numbering of (**a**) 6-chloro-7-propargylamine-5,8-quinolinedione **2a**; (**b**) 7-chloro-6-propargylamine-5,8-quinolinedione **3a**.

Table 1. Crystal parameters, data collection and refinement details for compounds **2a** and **3a**.

Parameter	2a	3a
Chemical formula	$C_{12}H_7ClN_2O_2$	$C_{12}H_7ClN_2O_2$
M_r	246.65	
Crystal system, space group	Monoclinic, *Pc*	Monoclinic, $P2_1/n$
Temperature (K)	100	
a, *b*, *c* (Å)	4.0250 (12), 6.5937 (6), 19.3214 (13)	11.1550 (3), 7.9114 (2), 12.0047 (3)
β (°)	90.673 (12)	97.554 (3)
V (Å^3)	512.75 (16)	1050.24 (5)
Z	2	4
Radiation type	Mo *Kα*	
μ (mm^{-1})	0.36	0.35
Crystal size (mm)	0.38 × 0.05 × 0.04	0.56 × 0.22 × 0.03
Diffractometer	Oxford Diffraction diffractometer with Sapphire3 detector	
Absorption correction	Multi-scan *CrysAlis RED*, Oxford Diffraction Ltd., Version 1.171.32.29 Empirical absorption correction using spherical harmonics, implemented in SCALE3 ABSPACK scaling algorithm.	
T_{min}, T_{max}	0.875, 0.984	0.911, 1.000
No. of measured, independent and observed [$I > 2\sigma(I)$] reflections	3745, 1261, 1144	7654, 1995, 1657
R_{int}	0.036	0.026
$(\sin\theta/\lambda)_{max}$ (Å^{-1})	0.609	0.610
$R[F^2 > 2\sigma(F^2)]$, $wR(F^2)$, *S*	0.032, 0.078, 1.00	0.027, 0.072, 1.03
No. of reflections	1261	1995
No. of parameters	164	160
No. of restraints	2	-
H-atom treatment	H atoms treated by a mixture of independent and constrained refinement	
$(\Delta)_{max}$, $(\Delta)_{min}$ (e Å^{-3})	0.61, −0.25	0.30, −0.20
Absolute structure	Refined as an inversion twin.	-
Absolute structure parameter	0.95 (14)	-

The selected values of bond distances and angles are presented in Table S1 (supplement material). In terms of bond distances and angles, the geometry of molecules **2a** and **3a** shows typical values [23,25]. These are in good agreement with the calculated values. The observed discrepancies between experimental and calculated values are mainly due to the method of calculations. They were done for a single molecule in a vacuum, which means that intermolecular interactions were not taken into account.

The unit cell of **2a** contains two molecules (Z = 2). The 5,8-quinolinedione rings accomplish a planar structure. In the unit cell these planes are arranged parallel to each other (see Figure S9 in supplement material). An angle between plane of rings and the propargylamine chain N2C9C10C11 is equal to 84.77°. This conformation is very similar to that which occurred for the corresponding angle in the crystal structure of the 6-chloro-7-propylamine-5,8-quinolinedione (89.77°) described earlier by Jastrzebska et al. [25]. Figure 2 depicts the hydrogen bonds found in the crystal structure of **2a**. In Table 2 parameters of the hydrogen bonds for **2a** are collected.

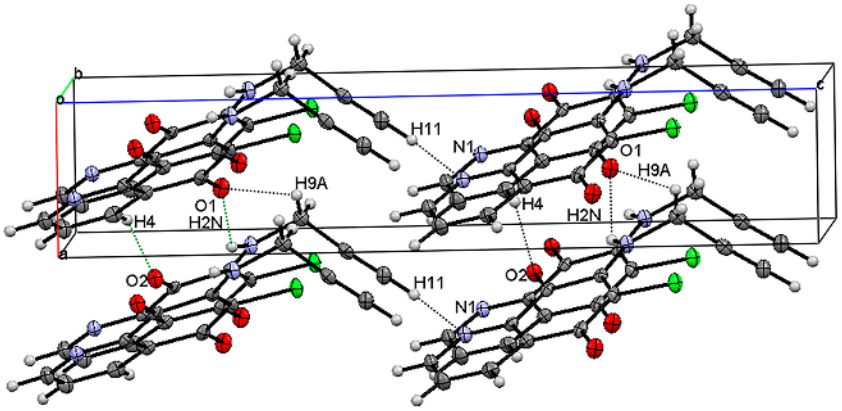

Figure 2. Crystal structure and hydrogen bonds for 6-chloro-7-propargylamine-5,8-quinolinedione **2a**.

Table 2. Parameters (Å, Degree) of the hydrogen bonds for compounds **2a** and **3a**.

D–H···A	D–H	H···A	D···A	<D–H···A
6-chloro-7-propargylamine-5,8-quinolinedione ***2a***				
C4–H4···O2	0.95 (1)	2.373 (4)	3.219 (4)	148.1
N2–H2N···O1	0.83 (1)	2.403 (4)	3.015 (4)	131.2
C9–H9A···O1	0.83 (2)	2.629 (2)	3.207 (2)	127.9
C11–H11···N1	0.95 (1)	2.300 (2)	3.158 (3)	149.9
7-chloro-6-propargylamine-5,8-quinolinedione ***3a***				
N2–H2N···N1	0.85 (1)	2.181 (1)	2.957 (1)	152.5
C11–H11···O2	0.95 (1)	2.338 (2)	3.282 (1)	172.2

Both carbonyl groups of **2a** participate in the formation of hydrogen bonds. The oxygen atom O1 forms the bifurcated hydrogen bond, which can be described as: N2–H2N···O1···H9A–C9 (Figure 2). Two other short hydrogen bonds C11–H11···N1 and C4–H4···O2 have also been found in **2a** with the H···A distances equal to 2.373 and 2.300 Å, respectively (Table 3). According to the literature data [26,27], for the hydrogen bonds from the acidic C–H donors in the C≡C–H to the N acceptors, the mean H···N distance is reported to be 2.40 Å. The reason for the shorter H···N distance in **2a** might be the higher basicity of the pyridyl N atom.

For the 7-chloro-6-propargylamine-5,8-quinolinedione **3a**, the crystal unit cell contains four molecules (Z = 4, Table 1). The molecules form two layers with the 5,8-quinolinedione rings located inside the unit (see Figure S10 in supplement material). An angle between the 5,8-quinolinedione rings' plane and the propargylamine chain is equal to 68.57° and is significantly smaller than that for **2a**

(84.77°). Simultaneously, this angle is very similar to the corresponding angle in the crystal structure of the 7-chloro-6-propylamine-5,8-quinolinedione **3e** (68.57°), which was described earlier [25]. Figure 3 shows the unit cell and the hydrogen bonds identified in the crystal structure of **3a**. All parameters of the H-bonds seen in Figure 3 are summarized in Table 2.

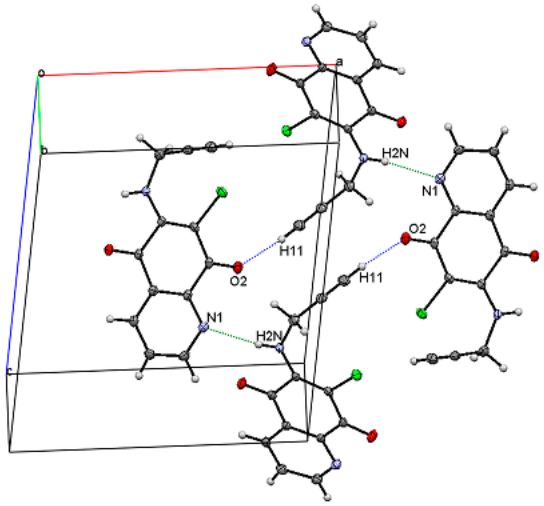

Figure 3. Crystal structure and hydrogen bonds in of 7-chloro-6-propargylamine-5,8-quinolinedione **3a**.

For **3a** crystal structure, the inter- and intra-molecular hydrogen bonds C11–H11···O1 and N2–H2N···N1 are observed, respectively. The N···N distance between the donor and acceptor nitrogen nuclei for the **3a** and **3e** are equal to 2.957 Å and 3.151 Å, respectively [25]. This pronounced difference could be explained by the higher basicity of the N–H donor group from the propargylamine chain in comparison to that from the propylamine.

2.3. IR Spectra

Analysis of the IR spectral bands, especially in the frequency ranges of the carbonyl and amine stretching vibrations, have been performed using the calculated harmonic vibrational spectra. Comparison of the experimental and the density functional theory (DFT)-calculated spectra allowed also to obtain information about an impact of the H-bond formation on the vibrational bands, e.g., ν_{str}(N–H), ν_{str}(C=O) or ν_{str}(C≡C–H).

In Figures 4 and 5, the IR spectra for compounds **2a** and **3a**, both experimental and calculated, are presented. Assignments of the selected bands for all spectra are shown in Table 3.

As shown in Figures 4 and 5, the calculated spectra well reproduce these experimental. This also gives good agreement between calculated and experimental frequencies, which can be seen in Table 3. The observed differences are mainly due to the fact that we are comparing the theoretical spectra of a single molecule in a vacuum with the experimental spectra of crystalline substance.

At lower wavenumbers, i.e., below 1300 cm^{-1}, the observed bands are mainly assigned to the aromatic C–C and C–H vibrations. One can also observe the C–C and C≡C–H aliphatic bend vibrations near 580–590 cm^{-1} and 650–660 cm^{-1}, respectively. For compound **2a** the band at 1427 cm^{-1} is assigned to the C–H aliphatic stretching vibrations. As is seen in Figure 4a, its experimental and calculated band intensities show significant difference. The higher intensity of the experimental band is due to formation of the hydrogen bond C9–H9A···O1. According to literature data [26–28], the enhancement of the band intensity for the stretching vibrations of the X–H group (H-bond donor group) is associated with the exceptionally great variation of the electric dipole moment of X–H···Y. This enhancement of intensity is sometimes used to extract information on H-bond [28].

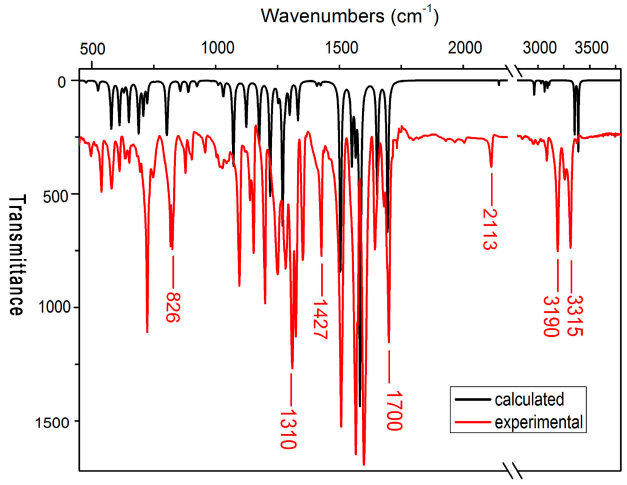

Figure 4. Experimental (red line) and calculated (black line) IR spectra for 6-chloro-7-propargylamine-5,8-quinolinedione **2a** (450–3500) cm^{-1}. See Table 3 for band assignments.

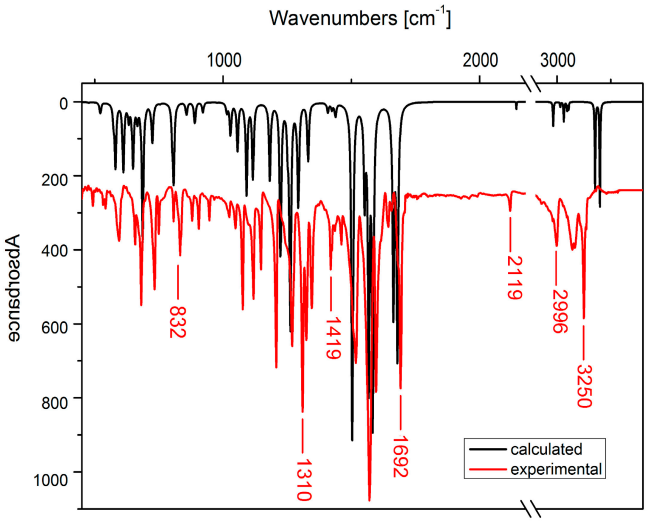

Figure 5. Experimental (red line) and calculated (black line) IR spectra for 7-chloro-6-propargylamine-5,8-quinolinedione **3a** (450–3500) cm^{-1}. See Table 3 for band assignments.

Table 3. Experimental and calculated vibrational frequencies (cm^{-1}) and band assignments for studied compounds **2a** and **3a**.

Experimental	Calculated	Assignment
6-chloro-7-propargylamine-5,8-quinolinedione **2a**		
581	579	C–C aliphatic bend
652	650	C≡C–H bend
748–696	723–689	C–C ring stretch, C–H ring stretch
826–818	803	C–Cl bend
1153–1139	1175–1123	C–C ring bend, C–H ring bend
1120	1220	HN–C ring bend, C–H ring bend
1283–1250	1272	C–C ring stretch
1332–1310	1299	C–C ring bend
1353	1332	C–H aliphatic bend
1427	1423	C–H aliphatic stretch
1506	1504	N–H bend
1599–1565	1534–1550	C–H ring bend, C–H aliphatic stretch
1643	1652	C=O sym stretch

Table 3. *Cont.*

Experimental	Calculated	Assignment
6-chloro-7-propargylamine-5,8-quinolinedione ***2a***		
1700 1680	1695	C=O asym stretch, N–H bend
2113	2145	C≡C stretch
2957	2964	C–H aliphatic stretch
3085–3038	3109–3064	C–H ring stretch
3190	3354	C≡CH stretch
7-chloro-6-propargylamine-5,8-quinolinedione ***3a***		
595	611–580	C–C aliphatic bend
657	657	C≡C–H bend
749–681	725–687	C–C ring stretch, C–H ring stretch
832–807	806	C–Cl bend
1147–1076	1182–1091	C–C ring bend, C–H ring bend
1207	1224	HN–C ring bend, C–H ring bend
1269	1261	C–C ring stretch
1324–1310	1293	C–C ring bend
1346	1331	C–H aliphatic bend
1419	1407	C–H aliphatic stretch
1461	1438	C–H ring bend, C–C ring bend
1517	1503	N–H bend
1597–1569	1584–1551	C–H ring bend, C–H aliphatic stretch
1682	1664	C=O sym stretch, N–H bend
1692	1679	C=O asym stretch
2119	2143	C≡C stretch
2996	2965	C–H aliphatic stretch
3168–3058	3108–3030	C–H ring stretch
3250	3354	C≡CH stretch
3271	3399	N–H stretch

In Figure 6, the experimental and calculated IR spectra in the range of the carbonyl bands ~1600–1750 cm^{-1} are exposed. Each molecule of **2a** and **3a** possess two carbonyl groups in the para position. Stretching vibrations of two carbonyl groups are usually coupled into two vibrations located at different frequencies, i.e., asymmetric (out of phase) ν_{as} at higher frequency and symmetric (in phase) ν_s at lower frequency (see Table 3).

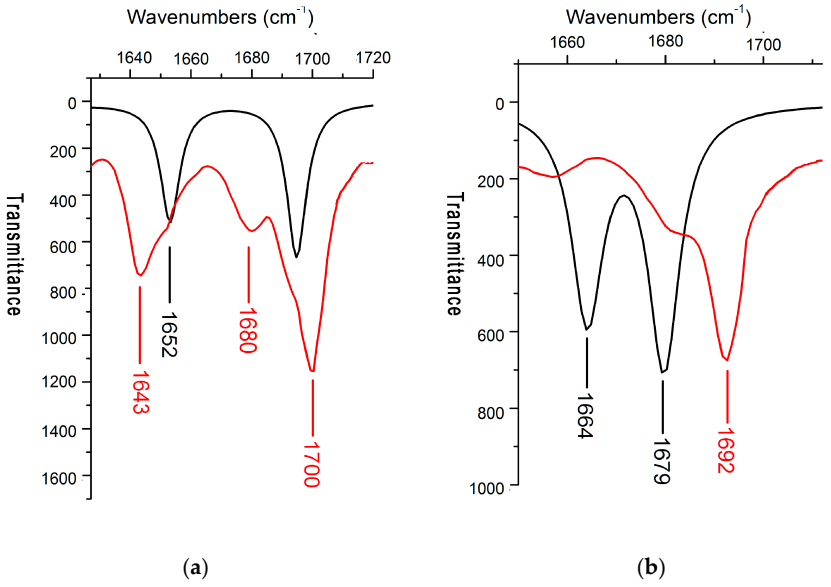

Figure 6. Experimental (red line) and calculated (black line) IR spectra showing carbonyl bands for (**a**) 6-chloro-7-propargylamine-5,8-quinolinedione **2a**; and (**b**) 7-chloro-6-propargyl-5,8-quinolinedione **3a**.

Analysis of the calculated spectra revealed the band ν_{as} is attributed mainly to the carbonyl vibration at the C-8 atom, whereas the ν_s band is attributed to the C=O vibrations at the C-5 atom. Furthermore, for the 7-substituted derivative, the N–H bending is involved in the ν_{as} carbonyl stretching, while for the 6-substituted derivative, the N–H bending is involved in the ν_s carbonyl vibrations. A very similar situation occurred for the 6- and 7-propylamine-substituted 5,8-quinolinedione derivatives described previously by Jastrzebska et al. [25]. As in this case, the C=O stretching and the N–H bending vibrations showed coupling effect if they were positioned in close proximity within the molecule. Moreover, there is a correlation between the frequency separation $\Delta\nu = \nu_{as} - \nu_s$ of the carbonyl bands and the position of the substituent, i.e., the 7-substituted derivative shows higher value of $\Delta\nu$ than the 6-substituted one. For the 7-propargylamine-substituted 5,8-quinolinedione the calculated and experimental separation values $\Delta\nu$ are 57 cm^{-1} and 43 cm^{-1} versus 10 cm^{-1} and 15 cm^{-1} for the 6-substituted derivative, respectively (see Table 3). The similar situation occurred in the case of the 7- and 6-propylamine-substituted 5,8-quinolinediones described previously [25], for which the $\Delta\nu$ were 59 cm^{-1} and 51 cm^{-1} versus 31 cm^{-1} and 7 cm^{-1} for the 7- and 6-substituted derivatives, respectively.

For the 7-propargylamino-5,8-quinolinedione **2a**, the ν_{as} stretching band shows two peaks at 1700 and 1680 cm^{-1} (see Figure 5), while for the 6-substituted derivative **3a** only single peak at 1692 cm^{-1} is observed. This effect can be due to the formation of the bifurcated H-bond N2–H2N···O1···H9A–C9 described in the previous subsection. The N–H group of the propargylamine chain is involved in both the bifurcated H-bond and the ν_{as} carbonyl stretching vibrations at the C-8 atom. It is also worth noting that the observed splitting into two peaks at 1700 and 1680 cm^{-1} for the ν_{as} stretching band of the 7-substituted derivative is probably not associated with the type of interaction with the D-H system, but originates rather from the ν_{as} distinctive characteristics.

The bifurcated H-bond also strongly influences the N–H stretching vibrations, giving two peaks at the 3315 and 3258 cm^{-1}. For the 6-substituted propargylamine derivative, the bifurcated H-bond is absent giving only single band at 3250 cm^{-1} due to the N–H stretching vibrations.

2.4. Antiproliferative Activity

Compounds **1**, **2a–e** and **3a–e** were tested for the antiproliferative activity in vitro against the three human cancer cell lines: melanoma (C-32), glioblastoma (SNB-19) and breast cancer (T47D). Results of the analysis have been summarized in Table 4.

Table 4. Cytotoxic activity of 6,7-dichloro-5,8-quinolinedione **1**, amine derivatives of 5,8-quinolinedione **2–3** and cisplatin as a reference compound.

Compound	Cytotoxic Activity IC_{50} (μg/mL)		
	C-32	SNB-19	T47D
1	42.48 ± 2.02	2.77 ± 0.07	8.26 ± 0.32
2a	0.61 ± 0.02	0.26 ± 0.02	8.50 ± 0.54
2b	0.75 ± 0.05	0.97 ± 0.01	9.22 ± 0.77
2c	0.67 ± 0.01	0.98 ± 0.01	9.14 ± 0.77
2d	0.63 ± 0.02	0.88 ± 0.05	9.03 ± 0.10
2e	0.64 ± 0.03	0.50 ± 0.04	8.54 ± 0.41
3a	0.58 ± 0.03	0.09 ± 0.01	1.01 ± 0.05
3b	0.67 ± 0.05	0.44 ± 0.01	8.48 ± 0.55
3c	0.65 ± 0.05	0.92 ± 0.07	4.57 ± 0.62
3d	0.61 ± 0.03	0.79 ± 0.03	7.07 ± 0.28
3e	0.64 ± 0.01	0.28 ± 0.05	3.05 ± 5.65
cisplatin	1.51 ± 0.49	0.79 ± 0.07	62.65 ± 2.70

It is seen that introduction of the alkynyl, allyl and propyl chains at the C-7 or C-6 position leads to an increase in the cytotoxic activity for the (C-32) and (SNB-19) cell lines in comparison to

the 6,7-dichloro-5,8-quinolinedione **1**. Furthermore, the acetylenic amine derivatives **2a**–**c** and **3a**–**c** show higher activity than the reference compound cisplatin against the C-32 and T47D cell lines. All amino derivatives of the 5,8-quinolinedione show high cytotoxic activity against the melanoma (C-32) cell line, with the IC_{50} varying in the range 0.58 to 0.75 μg/mL. Comparing the activity of compounds with alkane (**2e** and **3e**), alkene (**2d** and **3d**) and alkyne (**2a** and **3a**) moiety, showed that the cytotoxic of derivatives depends on the type of bond in the substituent; the rank order of activity against the C-32 cell line, is as follows: propargyl > allyl > propyl. Moreover, for the other cell line (SNB-19 and T47D) the highest activity showed propargylamino compounds **2a** and **3a**. The activity of **3a** and **2a** against the glioblastoma (SNB-19) cell line for which the IC_{50} parameters have the lowest values 0.09 ± 0.01 μg/mL and 0.26 ± 0.02 μg/mL, respectively. These results suggested that the triple bond seems to be essential for anticancer activity.

For compounds with the acetylenic amine substituents, the cytotoxic activity against the melanoma (C-32) and the breast cancer (T47D) cell lines follows the order: *N*-methylpropargylamine < 1,1-dimethylpropargylamine < propargylamine. As one can see, expansion of the acetylenic amine chain by binding methyl groups gives a reduction of the cytotoxic activity.

3. Materials and Methods

3.1. General Techniques

Melting points were measured in the open capillary tubes on a Boetius melting point apparatus. NMR spectra (600/150 MHz) were registered on a Bruker Avance 600 spectrometer (Bruker, Billerica, MA, USA). The spectra were recorded for ^{1}H and ^{13}C NMR at room temperature. Chemical shifts were reported in ppm (ν) and *J* values in Hz. Multiplicity was designated as the singlet (s), doublet (d), triplet (t) and multiplet (m). High-resolution mass spectral analysis was carried out on a Bruker Impact II instrument (Bruker, Billerica, MA, USA) The infrared spectra (IR) were registered using the IRAffinity 1 spectrometer (Shimadzu, Japan) and the KBr pellet method for the sample preparation. All spectra were recorded in the range of 400–4000 cm^{-1} at room temperature. TLC was carried out on silica gel plates (Merck, Darmstadt, Germany) using a mixture of chloroform and ethanol as an eluent. The visualization was accomplished with UV light and iodine vapour. Column chromatography was performed on silica gel (Merck) with the mixture of chloroform and ethanol (40:1, *v*/*v*) as an eluent.

3.2. Chemistry

The 6,7-dichloro-5,8-quinolinedione **1** was synthesized from the 8-hydroxyquinoline according to the method described in the literature [12].

Synthesis of the 6-chloro-7-substituted-5,8-quinolinediones **2a**–**e** and 7-chloro-6-substituted-5,8-quinolinediones **3a**–**e** was as follows:

Synthesis was carried out using the procedure previously described by Kadela et al. [8,9,25]. Briefly, the 6,7-dichloro-5,8-quinolinedione **1** (0.1 g, 0.441 mmol) was dissolved in dry tetrahydrofuran (1 mL). Next, the potassium carbonate (0.061 g, 0.441 mmol) and corresponding amine (0.441 mmol) were added to the mixture. After 3 h of stirring at room temperature, the solvent was removed under reduced pressure. The residue was purified by the column chromatography ($CHCl_3$/EtOH, 40:1 *v*/*v*) to give pure products **2** and **3**.

6-chloro-7-propargylamine-5,8-quinolinedione ***2a*** Yield 68%; mp 140–142 °C; ^{1}H NMR ($CDCl_3$, 600 MHz) δ 2.42 (t, *J* = 2.4 Hz, 1H, CH), 4.68 (dd, *J* = 2.4 Hz, 2H, CH_2), 6.19 (t, 1H, NH), 7.68 (dd, J_{23} = 4.8 Hz, J_{34} = 7.8 Hz, 1H, H-3), 8.47 (dd, J_{24} = 1.8 Hz, J_{34} = 7.8 Hz, 1H, H-4), 8.96 (dd, J_{24} = 1.8 Hz, J_{23} = 4.8 Hz, 1H, H-2). ^{13}C NMR ($CDCl_3$, 150 MHz) δ ppm: 35.1 ($\underline{C}H_2$), 73.8 (C≡$\underline{C}$H), 78.8 ($\underline{C}$≡CH), 128.4 (C-6), 129.5 (C-3), 129.7 (C-4a), 134.8 (C-4), 143.9 (C-7), 145.9 (C-8a), 153.7 (C-2), 165.4 (C-8), 178.4 (C-5). IR (KBr) ν_{max} (cm^{-1}) 3315–3258 (N–H), 3190–3038 (C–H), 2113 (C≡C), 1700 (C=O), 1643 (C=O), 1599–1565 (C–H). HRMS (APCI) *m*/*z* 247.0265 (calcd for $C_{12}H_8ClN_2O_2$, 247.0274).

6-chloro-7-(N-methylpropargylamine)-5,8-quinolinedione ***2b*** Yield 61%; mp 130–132 °C; ^{1}H NMR ($CDCl_3$, 600 MHz) δ 2.38 (t, *J* = 2.4 Hz, 1H, CH), 3.32 (s, 3H, CH_3), 4.33 (d, *J* = 2.4 Hz, 2H, CH_2), 7.65 (dd, J_{23} = 4.8 Hz, J_{34} = 7.8 Hz, 1H, H-3), 8.46 (dd, J_{24} = 1.8 Hz, J_{34} = 7.8 Hz, 1H, H-4), 8.97 (dd, J_{24} = 1.8 Hz, J_{23} = 4.8 Hz, 1H, H-2); ^{13}C NMR ($CDCl_3$, 150 MHz) δ 41.8 (CH_2), 44.8 (CH_3), 73.5 (C≡<u>C</u>H), 78.6 (<u>C</u>≡CH), 123.2 (C-6), 128.4 (C-3), 128.4 (C-4a), 134.6 (C-4), 147.1 (C-8a), 150.7 (C-7), 154.2 (C-2), 177.2 (C-8), 180.1 (C-5); IR (KBr) ν_{max} (cm^{-1}) 3360–3280 (N–H), 3036–2855 (C–H), 2117 (C≡C), 1692 (C=O), 1680 (C=O), 1588–1558 (C–H). HRMS (APCI) *m/z* 261.0420 (calcd for $C_{13}H_{10}ClN_2O_2$, 261.0431).

6-chloro-7-(1,1-dimethylpropargylamine)-5,8-quinolinedione ***2c*** Yield 58%; mp 156–157 °C; ^{1}H NMR ($CDCl_3$, 600 MHz) δ 1.88 (s, 6H, CH_3, CH_3), 2.45 (t, *J* = 2.4 Hz, 1H, CH), 6.03 (s, 1H, NH), 7.66 (dd, J_{23} = 4.8 Hz, J_{34} = 7.8 Hz, 1H, H-3), 8.46 (dd, J_{24} = 1.8 Hz, J_{34} = 7.8 Hz, 1H, H-4), 8.95 (dd, J_{24} = 1.8 Hz, J_{23} = 4.8 Hz, 1H, H-2); ^{13}C NMR ($CDCl_3$, 150 MHz) δ 29.7 (CH_3), 32.8 (CH_3), 51.1 (NH<u>C</u>), 72.3 (C≡<u>C</u>H), 86.6 (<u>C</u>≡CH), 126.1 (C-6), 128.1 (C-3), 129.1 (C-4a), 134.6 (C-4), 145.6 (C-8a), 146.4 (C-7), 153.7 (C-2), 176.0 (C-8), 178.5 (C-5); IR (KBr) ν_{max} (cm^{-1}) 3367–3241 (N–H), 2926–2871 (C–H), 2113 (C≡C), 1700 (C=O), 1683 (C=O), 1653–1635 (C–H). HRMS (APCI) *m/z* 275.0577 (calcd for $C_{14}H_{12}ClN_2O_2$, 275.0587).

6-chloro-7-allylamine-5,8-quinolinedione ***2d*** Yield 65%; mp 122–123 °C; ^{1}H NMR ($CDCl_3$, 600 MHz) δ 4.53 (dt, *J* = 1.2 Hz, *J* = 6.0 Hz, 2H, $NHCH_2$), 5.30 (dt, *J* = 1.2 Hz, *J* = 9.0 Hz, 2H, CH=<u>CH_2</u>), 6.00 (m, 1H, <u>CH</u>=CH_2), 6.25 (s, 1H, NH), 7.66 (dd, J_{23} = 4.8 Hz, J_{34} = 7.8 Hz, 1H, H-3), 8.48 (dd, J_{24} = 1.8 Hz, J_{34} = 7.8 Hz, 1H, H-4), 8.93 (dd, J_{24} = 1.8 Hz, J_{23} = 4.8 Hz, 1H, H-2); ^{13}C NMR ($CDCl_3$, 150 MHz) δ 47.2 ($NHCH_2$), 117,9 (CH=<u>CH_2</u>), 128.2 (C-6), 128.3 (C-3), 129.7 (C-4a), 134.7 (<u>CH</u>=CH_2), 135.6 (C-4), 144.4 (C-8a), 146.8 (C-7), 155.4 (C-2), 176.3 (C-8), 178.8 (C-5); IR (KBr) ν_{maxx} (cm^{-1}) 3304 (N–H), 2957–2854 (C–H), 1693 (C=O), 1680 (C=O), 1598–1560 (C–H); HRMS (APCI) *m/z* 261.0425 (calcd for $C_{12}H_{10}ClN_2O_2$, 249.0431).

7-chloro-6-propargylamine-5,8-quinolinedione ***3a*** Yield 19%; mp 140–142 °C; ^{1}H NMR ($CDCl_3$, 600 MHz) δ 2.37 (t, *J* = 2.4 Hz, 1H, CH), 4.67 (dd, *J* = 2.4 Hz, 2H, CH_2), 6.01 (t, 1H, NH), 7.62 (dd, J_{23} = 4.8 Hz, J_{34} = 7.8 Hz, 1H, H-3), 8.37 (dd, J_{24} = 1.8 Hz, J_{34} = 7.8 Hz, 1H, H-4), 9.03 (dd, J_{24} = 1.8 Hz, J_{23} = 4.8 Hz, 1H, H-2); ^{13}C NMR ($CDCl_3$, 150 MHz) δ 35.1 (<u>C</u>H_2), 73.7 (C≡<u>C</u>H), 78.9 (<u>C</u>≡CH), 126.8 (C-6), 130.2 (C-3), 131.0 (C-4a), 133.7 (C-4), 143.1 (C-7), 148.0 (C-8a), 155.3 (C-2), 165.4 (C-8), 179.7 (C-5); IR (KBr) ν_{max} (cm^{-1}) 3271 (N–H), 3250–3058 (C–H), 2119 (C≡C), 1692 (C=O), 1682 (C=O), 1597–1569 (C–H); HRMS (APCI) *m/z* 247.0263 (calcd for $C_{12}H_8ClN_2O_2$, 247.0274).

7-chloro-6-(N-methylpropargylamine)-5,8-quinolinedione ***3b*** Yield 21%; mp 126–127 °C; ^{1}H NMR ($CDCl_3$, 600 MHz) δ 2.39 (t, *J* = 2.4 Hz, 1H, CH), 3.31 (s, 3H, CH_3), 4.29 (d, *J* = 2.4 Hz, 2H, CH_2), 7.63 (dd, J_{23} = 4.8 Hz, J_{34} = 7.8 Hz, 1H, H-3), 8.38 (dd, J_{24} = 1.8 Hz, J_{34} = 7.8 Hz, 1H, H-4), 9.01 (dd, J_{24} = 1.8 Hz, J_{23} = 4.8 Hz, 1H, H-2); ^{13}C NMR ($CDCl_3$, 150 MHz) δ 41.7 (CH_2), 44.7 (CH_3), 73.4 (C≡<u>C</u>H), 78.8 (<u>C</u>≡CH), 125.3 (C-7), 127.2 (C-3), 129.7 (C-4a), 135.0 (C-4), 147.2 (C-8a), 149.5 (C-6), 155.3 (C-2), 176.6 (C-8), 181.3 (C-5); IR (KBr) ν_{max} (cm^{-1}) 3175 (N–H), 2927–2854 (C–H), 2107 (C≡C), 1674 (C=O), 1592–1520; HRMS (APCI) *m/z* 261.0422 (calcd for $C_{13}H_{10}ClN_2O_2$, 261.0431).

7-chloro-6-(1,1-dimethylpropargylamine)-5,8-quinolinedione ***3c*** Yield 16%; mp 148–149 °C; ^{1}H NMR ($CDCl_3$, 600 MHz) δ 1.86 (s, 6H, CH_3, CH_3), 2.44 (t, *J* = 2.4 Hz, 1H, CH), 5.85 (s, 1H, NH), 7.61 (dd, J_{23} = 4.8 Hz, J_{34} = 7.8 Hz, 1H, H-3), 8.39 (dd, J_{24} = 1.8 Hz, J_{34} = 7.8 Hz, 1H, H-4), 9.02 (dd, J_{24} = 1.8 Hz, J_{23} = 4.8 Hz, 1H, H-2); ^{13}C NMR ($CDCl_3$, 150 MHz) δ 29.5 (CH_3), 32.7 (CH_3), 51.3 (NH<u>C</u>), 72.2 (C≡<u>C</u>H), 86.5 (<u>C</u>≡CH), 127.4 (C-7), 128.2 (C-3), 129.0 (C-4a), 134.4 (C-4), 145.5 (C-8a), 147.5 (C-6), 153.5 (C-2), 177.1 (C-8), 182.1 (C-5); IR (KBr) ν_{max} (cm^{-1}) 3316 (N–H), 3154–2963 (C–H), 2100 (C≡C), 1685 (C=O), 1653 (C=O), 15989–1560 (C–H); HRMS (APCI) *m/z* 275.0575 (calcd for $C_{14}H_{12}ClN_2O_2$, 275.0587).

7-chloro-6-allylamine-5,8-quinolinedione ***3d*** Yield 20%, mp 139–141 °C. ^{1}H NMR ($CDCl_3$, 600 MHz) δ 4.51 (dt, *J* = 1.2 Hz, *J* = 6.0 Hz, 2H, $NHCH_2$), 5.29 (dt, *J* = 1.2 Hz, *J* = 9.0 Hz, 2H, CH=<u>CH_2</u>), 5.99 (m, 1H, <u>CH</u>=CH_2), 6.15 (s, 1H, NH), 7.59 (dd, J_{23} = 4.8 Hz, J_{34} = 7.8 Hz, 1H, H-3), 8.67 (dd, J_{24} = 1.8 Hz, J_{34} = 7.8 Hz, 1H, H-4), 9.01 (dd, J_{24} = 1.8 Hz, J_{23} = 4.8 Hz, 1H, H-2); ^{13}C NMR ($CDCl_3$, 150 MHz) δ 47.2 ($NHCH_2$), 117,8 CH=<u>CH_2</u>), 126.5 (C-7), 126.8 (C-3), 129.7 (C-4a), 134.8 (<u>CH</u>=CH_2), 134.6 (C-4),

147.4 (C-8a), 148.4 (C-6), 155.3 (C-2), 178.3 (C-8), 180.0 (C-5); IR (KBr) ν_{max} (cm^{-1}) 3321 (N–H), 3080–2926 (C–H), 1683 (C=O), 1647 (C=O), 1602–1559 (C–H); HRMS (APCI) *m/z* 261.0424 (calcd for $C_{12}H_{10}ClN_2O_2$, 249.0431).

6-chloro-7-propylamine-5,8-quinolinedione **2e** and 6-chloro-7-propylamine-5,8-quinolinedione **3e**: the spectral data were previously described in the literature [25].

3.3. X-ray Diffraction

The single crystal X-ray experiment was carried out for the following two compounds: 6-chloro-7-propargylamine-5,8-quinolinedione **2a** and 7-chloro-6-propargylamine-5,8-quinolinedione **3a**, at 100.0(1) K. Single crystals of both compounds were preselected under microscope. The crystals were installed on a glass capillary and cooled down by Cryostream Cooler (Oxford Cryosystems Ltd, Oxford, UK). Data sets were collected using an Oxford Diffraction κ diffractometer with a Sapphire3 CCD detector (Oxford Diffraction Ltd., Yarnton, UK). For the integration of the collected data, the CrysAlis RED software (version 1.171.32.29, Agilent Technologies) was applied. The crystal structures were solved using direct methods with the SHELXS-97 software. The solutions were refined using SHELXL-97, SHELXS-2014, and SHELXL-2014/6 programs [29].

The supplementary crystallographic data for **2a** and **3a** were deposited at the Cambridge Crystallographic Data Centre (CCDC) as CCDC-1047971 and CCDC-104797. These data can be obtained free of charge from the CCDC via www.ccdc.cam.ac.uk/data_request/cif.

3.4. Density Functional Theory (DFT) Analysis

Harmonic vibrational spectra were calculated by the DFT method implemented in the Gaussian09 software package [30]. Details have been described in the earlier work [25]. Briefly, the ground state molecular structure was optimized in silico using the B3LYP exchange-correlation functional with the 6-31+G(d,p) basis set. The initial molecular structures of compounds **2a** and **3a** were taken from the X-ray crystallographic data. The obtained harmonic frequencies were scaled by a factor of 0.964 in accordance with [31]. Calculated vibrational modes were also analyzed using the GaussView 5.0 visualization software (Gaussian, Inc., Wallingford, CT, USA). The effect of the position of 6- and 7-propargylamine chain on carbonyl vibrations was observed by taking into account the displacement vectors.

3.5. Antiproliferative Assay In Vitro

3.5.1. Cell Culture

All compounds **1**, **2a**–**e** and **3a**–**e** were screened for antiproliferative activity using three cultured cell lines: SNB-19 (human glioblastoma, DSMZ-German Collection of Microorganisms and Cell Cultures, Braunschweig, Germany), C-32 (human amelanotic melanoma, ATCC-American Type Culture Collection, Manassas, VA, USA) and T47D (human ductal breast epithelial tumor cell line, ATCC, Manassas, VA, USA). The cultured cells were kept at 37 °C in the 5% CO_2 atmosphere. The cells were seeded (1×10^4 cells/well/100 µL Dulbecco's modified Eagle's medium (DMEM) supplemented with 10% fetal calf serum (FCS), streptomycin and penicillin) using the 96-well plates (Corning Inc., Corning, NY, USA).

3.5.2. Analysis of Antiproliferative Activity

The cytotoxic activities of tested compounds were determined using the Cell Proliferation Reagent WST-1 assay (Roche Diagnostics, Mannheim, Germany). The entire procedure was previously described in detail in an earlier work [8]. Cells were exposed to tested compounds for 24 h at indicated concentrations (in the rank of 0.1–100 µg/mL of dimethyl sulfoxide (DMSO)), and their viabilities were quantified using a cell proliferation assay. The WST-1-formazan was detected using a microplate reader

at 450 nm with the reference wavelength of 600 nm. Results were expressed as a mean value of at least three independent experiments performed in triplicate. The cytotoxic activity of the tested compound was compared to the cisplatin. The experiments were repeated in triplicate for each concentration of the compound. The IC_{50} parameter describes the concentration of compound (in μg/mL) that inhibits the proliferation rate of the tumor cells by 50% as compared to the control untreated cells. Calculation of the IC_{50} was performed using the GraphPad Prism 6 software (GraphPad Software, San Diego, CA, USA).

4. Conclusions

New 6- and 7-propargylamine-substituted 5,8-quinolinediones were synthesized and examined using the X-ray diffraction and IR spectroscopy supplemented by the density functional theory (DFT) calculations. Different positions of the propargylamine chain influenced crystal structure and formation of H-bonds. It was found that the H-bond distinctly affected the ν_{as} stretching band of the carbonyl groups only for the 7-propargylamine-substituted 5,8-quinolinedione.

Substantial changes in the frequency separation $\Delta\nu$ of the carbonyl stretching bands for different positions of the propargylamine chain were found. Higher frequency separation $\Delta\nu$ corresponds to the 7-substituted derivative. Correlation between the $\Delta\nu$ and position of substituent may provide an opportunity to use the IR spectroscopy to study substitution reaction.

Cytotoxic activities against three human cancer cell lines for the 5,8-quinolinedione derivatives with different amine substituents, i.e., propargylamine, *N*-methylpropargylamine, 1,1-dimethylpropargylamine, allylamine and propylamine were analyzed with respect to their molecular structure. It was found that introduction of the acetylenic, allyl and propylamine chains at the C-7 or C-6 position led to an increase in the cytotoxic activity for the melanoma and glioblastoma cell lines in comparison to the starting compound 6,7-dichloro-5,8-quinolinedione **1**. Furthermore, for the melanoma (C-32) and breast cancer (T47D) cell lines, the acetylenic amine derivatives showed higher activity than the reference compound cisplatin. The low IC_{50} values for the 7- and 6-substituted propargylamine derivatives against the glioblastoma (SNB-19) cell line were observed.

Supplementary Materials: The following are available online at www.mdpi.com/2073-4352/7/1/15/s1. Table S1: Selected geometric parameters given by X-ray diffraction experiment and theoretical calculations for compounds **2a** and **3a**. Figure S1: 6-chloro-7-propargylamine-5,8-quinolinedione **2a**, (a) ^{1}H NMR spectrum, (b) ^{13}C NMR spectrum, (c) IR spectrum. Figure S2: 6-chloro-7-(*N*-methylpropargylamine)-5,8-quinolinedione **2b**, (a) ^{1}H NMR spectrum, (b) ^{13}C NMR spectrum, (c) IR spectrum. Figure S3: 6-chloro-7-(1,1-dimethylpropargylamine)-5,8-quinolinedione **2c**, (a) ^{1}H NMR spectrum, (b) ^{13}C NMR spectrum, (c) IR spectrum. Figure S4: 6-chloro-7-allylamine-5,8-quinolinedione **2d**, (a) ^{1}H NMR spectrum, (b) ^{13}C NMR spectrum, (c) IR spectrum. Figure S5: 7-chloro-6-propargylamine-5,8-quinolinedione **3a**, (a) ^{1}H NMR spectrum, (b) ^{13}C NMR spectrum, (c) IR spectrum. Figure S6: 7-chloro-6-(*N*-methylpropargylamine)-5,8-quinolinedione **3b**, (a) ^{1}H NMR spectrum, (b) ^{13}C NMR spectrum, (c) IR spectrum. Figure S7: 7-chloro-6-(1,1-dimethylpropargylamine)-5,8-quinolinedione **3c**, (a) ^{1}H NMR spectrum, (b) ^{13}C NMR spectrum, (c) IR spectrum. Figure S8: 7-chloro-6-allylamine-5,8-quinolinedione **3d**, (a) ^{1}H NMR spectrum, (b) ^{13}C NMR spectrum, (c) IR spectrum. Figure S9: The crystal packing of 6-chloro-7-propargylamine-5,8-quinolinedione **2a**. View along axis "b". Figure S10: The crystal packing of 7-chloro-6-propargylamine-5,8-quinolinedione **3a**. View along axis "b".

Acknowledgments: This work was supported by the Medical University of Silesia in Katowice, Poland. Grant No. KNW-1-006/K/6/O and KNW-2-008/N/6/N.

Author Contributions: Monika Kadela-Tomanek and Stanisław Boryczka developed the concept of the work. Monika Kadela-Tomanek carried out the synthetic work and interpreted the results. Ewa Bębenek and Elwira Chrobak contributed to the synthesis and purification all new compounds. Maria Jastrzębska and Dorota Tarnawska participated in IR spectra interpretation. Małgorzata Latocha conducted a study of the biological activity. Joachim Kusz performed the X-ray analysis. Monika Kadela-Tomanek wrote the paper. All authors have given approval to the final version of the manuscript.

Conflicts of Interest: The authors declare no conflict of interest.

References

1. Bringmann, G.; Reichert, Y.; Kane, V.V. The total synthesis of streptonigrin and related antitumor antibiotic natural products. *Tetrahedron* **2004**, *60*, 3539–3574. [CrossRef]
2. Boger, D.L.; Yasuda, M.; Mitscher, L.A.; Drake, S.D.; Kitos, P.A.; Thompson, S.C. Streptonigrin and lavendamycin partial structures. Probes for the minimum, potent pharmacophore of streptonigrin, lavendamycin, and synthetic quinoline-5,8-diones. *J. Med. Chem.* **1987**, *30*, 1913–1928. [CrossRef]
3. Fryatt, T.; Goroski, D.T.; Nilson, Z.D.; Moody, C.J.; Beall, H. Novel quinolinequinone antitumor agents: Structure-metabolism studies with NAD(P)H:quinone oxidoreductase (NQO1). *Bioorg. Med. Chem. Lett.* **1999**, *9*, 2195–2198. [CrossRef]
4. Leteurtre, F.; Kohlhagen, G.; Pommier, Y. Streptonigrin induced topoisomerase II sites exhibit base preferences in the middle of the enzym stragger. *Biochem. Biophys. Res. Commun.* **1994**, *203*, 1259–1267. [CrossRef] [PubMed]
5. Kim, Y.-S.; Park, S.-Y.; Lee, H.-J.; Suh, M.-E.; Schollmeyer, D.; Lee, C.-O. Synthesis and cytotoxicity of 6,11-dihydro-pyrido- and 6,11-dihydro-benzo[2,3-b]phenazine-6,11-dione derivatives. *Bioorg. Med. Chem.* **2003**, *11*, 1709–1714. [CrossRef]
6. Alfadhli, A.; Mack, A.; Harper, L.; Berk, S.; Ritchie, C.; Barklis, E. Analysis of quinolinequinone reactivity, cytotoxicity, and anti-HIV-1 properties. *Bioorg. Med. Chem.* **2016**, *24*, 5618–5625. [CrossRef] [PubMed]
7. Ryu, C.-K.; Song, A.L.; Hong, J.A. Synthesis and antifungal evaluation of 7-arylamino-5,8-dioxo-5,8-dihydroisoquinoline-4-carboxylates. *Bioorg. Med. Chem. Lett.* **2013**, *23*, 2065–2068. [CrossRef] [PubMed]
8. Kadela, M.; Jastrzębska, M.; Bębenek, E.; Chrobak, E.; Latocha, M.; Kusz, J.; Książek, M.; Boryczka, S. Synthesis, structure and cytotoxic activity of mono- and dialkoxy derivatives of 5,8-quinolinedione. *Molecules* **2016**, *21*, 156. [CrossRef] [PubMed]
9. Kadela-Tomanek, M.; Jastrzębska, M.; Pawełczak, B.; Bębenek, E.; Chrobak, E.; Latocha, M.; Książek, M.; Kusz, J.; Boryczka, S. Alkynyloxy derivatives of 5,8-quinolinedione: Synthesis, in vitro cytotoxicity studies and computational molecular modeling with NAD(P)H:quinone oxidoreductase 1. *Eur. J. Med. Chem.* **2017**, *126*, 969–982. [CrossRef] [PubMed]
10. Rhee, H.K.; Park, H.J.; Lee, S.K.; Lee, C.-O.; Choo, H.-Y. Synthesis, cytotoxicity and DNA topoisomerase II inhibitory activity of benzofuroquinolinediones. *Bioorg. Med. Chem.* **2007**, *15*, 1651–1658. [CrossRef] [PubMed]
11. Ryu, C.-K.; Jeong, H.J.; Lee, S.K.; You, H.-J.; Chio, K.U.; Shim, J.-Y.; Heo, Y.-H.; Lee, C.-O. Effects of 6-arylamine-5,8-quinolinediones and 6-chloro 7-arylo-5,8-isoquinolinediones on NAD(P)H:quinone oxidoreductase (NQO1) activity and their cytotoxic potential. *Arch. Pharm. Res.* **2001**, *24*, 390–396. [CrossRef] [PubMed]
12. Mulchin, B.J.; Newton, C.G.; Baty, J.W.; Grasso, C.H.; Martin, W.J.; Walton, M.C.; Dangerfield, E.M.; Plunkett, C.H.; Berridge, M.V.; Harper, J.L.; et al. The anti-cancer, anti-inflammatory and tuberculostatic activities of a series of 6,7-substituted-5,8-quinolinequinones. *Bioorg. Med. Chem.* **2010**, *18*, 3238–3251. [CrossRef] [PubMed]
13. Yoon, E.Y.; Choi, H.Y.; Shin, K.J.; Yoo, K.H.; Chi, D.Y.; Kim, D.J. The regioselectivity in the reaction of 6,7-dihaloquinoline-5,8-diones with amine nucleophiles in various solvents. *Tetrahedron Lett.* **2000**, *41*, 7475–7480. [CrossRef]
14. Yin, H.; Kong, F.; Wang, S.; Yao, Z.-Y. Assembly of pentacyclic pyrido[4,3,2-mn]acridin-8-ones via a domino reaction initiated by Au(I)-catalyzed 6-endo-dig cycloisomerization of *N*-propargylaminoquinones. *Tetrahedron Lett.* **2012**, *53*, 7078–7082. [CrossRef]
15. Mól, W.; Matyja, M.; Filip, B.; Wietrzyk, J.; Boryczka, S. Synthesis and antiproliferative activity in vitro of novel (2-butynyl)thioquinolines. *Bioorg. Med. Chem.* **2008**, *16*, 8136–8141. [CrossRef] [PubMed]
16. Mól, W.; Naczyński, A.; Boryczka, S.; Wietrzyk, J.; Opolski, A. Synthesis and antiproliferative activity in vitro of diacetylenic thioquinolines. *Pharmazie* **2006**, *61*, 742–746. [PubMed]
17. Boryczka, S.; Bębenek, E.; Wietrzyk, J.; Kempińska, K.; Jastrzębska, M.; Kusz, J.; Nowak, M. Synthesis, structure and cytotoxic activity of new acetylenic derivatives of betulin. *Molecules* **2013**, *18*, 4526–4543. [CrossRef] [PubMed]

18. Marciniec, K.; Latocha, M.; Boryczka, S.; Kurczab, R. Synthesis, molecular docking study, and evaluation of the antiproliferative action of a new group of propargylthio- and propargylselenoquinolines. *Med. Chem. Res.* **2014**, *23*, 3468–3477. [CrossRef]
19. Siddiq, A.; Dembitsky, V. Acetylenic anticancer agents. *Anti-Cancer Agents Med. Chem.* **2008**, *8*, 132–170. [CrossRef]
20. Dembitsky, V.M.; Levitsky, D.O.; Gloriozovac, T.A.; Poroikovc, V.V. Acetylenic aquatic anticancer agents and related compounds. *Nat. Prod. Commun.* **2006**, *1*, 773–812.
21. Kuklev, D.V.; Dembitsky, V.M. Epoxy acetylenic lipids: their analogues and derivatives. *Prog. Lipid Res.* **2014**, *56*, 67–91. [CrossRef] [PubMed]
22. Kuklev, D.V.; Domb, A.J.; Dembitsky, V.M. Bioactive acetylenic metabolites. *Phytomedicine* **2013**, *20*, 1145–1159. [CrossRef] [PubMed]
23. Sun, S.; Tang, H.; Wu, P. Interpretation of carbonyl band splitting phenomenon of a novel thermotropic liquid crystalline polymer without conventional mesogens: Combination method of spectral analysis and molecular simulation. *J. Phys. Chem. B* **2010**, *114*, 3439–3448. [CrossRef] [PubMed]
24. Socrates, G. *Infrared Characteristic Group Frequencies*; John Wiley & Sons Inc.: New York, NY, USA, 1994.
25. Jastrzebska, M.; Boryczka, S.; Kadela, M.; Wrzalik, R.; Kusz, J.; Nowak, M. Synthesis, crystal structure and infrared spectra of new 6- and 7-propylamine-5,8-quinolinediones. *J. Mol. Struct.* **2014**, *1067*, 160–168. [CrossRef]
26. Desiraju, G.R.; Steiner, T. *The Weak Hydrogen Bond*; Oxford University Press: London, UK, 2006.
27. Steiner, T. The hydrogen bond in the solid state. *Angew. Chem.* **2002**, *41*, 48–79. [CrossRef]
28. Marechal, Y. *The Hydrogen Bond and the Water Molecule*; Elsevier: London, UK, 2007.
29. Sheldrick, G.M. A short history of SHELX. *Acta Cryst. A* **2008**, *64*, 112–122. [CrossRef] [PubMed]
30. Frisch, M.J.; Trucks, G.W.; Schlegel, H.B.; Scuseria, G.E.; Robb, M.A.; Cheeseman, J.R.; Scalmani, G.; Barone, V.; Mennucci, B.; Petersson, G.A.; et al. *Gaussian 09, Revision A. 02*; Gaussian Inc.: Wallingford, CT, USA, 2009.
31. NIST Computational Chemistry Comparison and Benchmark Database, NIST Standard Reference Database Number 101, Release 16a, August 2013, Editor: Russell D. Johnson III. Available online: http://cccbdb.nist.gov/ (accessed on 11 November 2015).